Massive stars dominate the production of ionizing photons, mechanical energy, and metals in the universe, ending their lives in nature's most energetic explosive events. Second only to the initial stellar mass, the principal parameter governing the evolutionary path of such stars is the amount of mass lost prior to the end of the nuclear burning. Yet, mass loss rates are still uncertain by factors approaching 100, with major discrepancies between theoretical and observational results. We propose a three-year program to initiate a novel method of measuring stellar mass loss rates while involving thousands of citizen scientists through the ***Zooniverse*** program in examining all-sky infrared images. Our cross-institutional team of students will carry out hands-on science over dozens of nights at the Wyoming Infrared Observatory 2.3 m telescope as they conduct a wide-area survey for high-velocity massive stars ejected from their birth environs. This collaboration between investigators at the rural University of Wyoming and Hispanic-serving Cal Poly Pomona will produce an all-sky sample of bowshock nebulae (**Figure 1**) and measure mass loss rates for their central O- and early B stars using a *new and physically independent* approach to help solve this vexing problem that touches nearly every area of contemporary astrophysics.

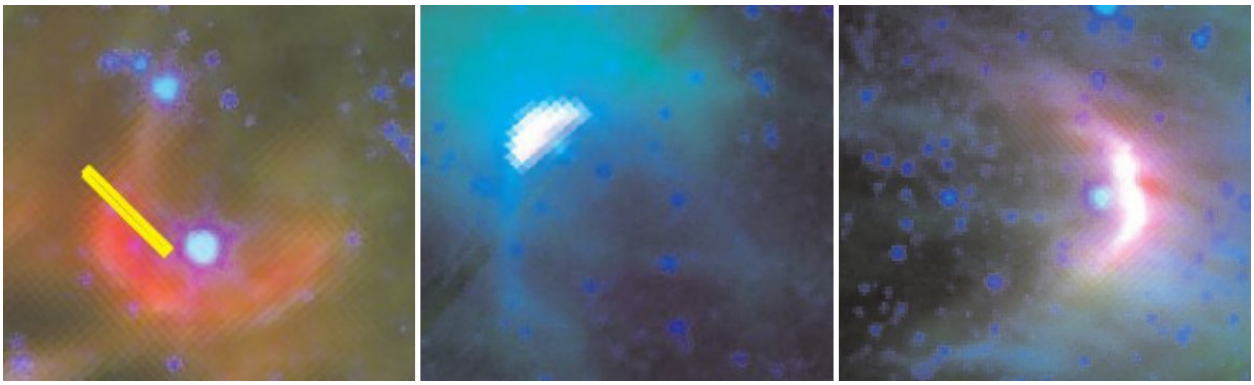

Figure 1 — Three examples of stellar bowshocks near the Cygnus OB2 Association (from Kobulnicky et al. 2010). Blue/green/red are the Spitzer 4.5/8.0/24 μm images. The yellow bar in the first panel shows the proper motion vector of this B0.2III star, consistent with a "runaway" threshold speed of ~25 km/s.

Figure 2 shows mass loss rates, in $M_\odot\,yr^{-1}$, for early type stars as a function of temperature class, with symbols coded by luminosity class (compiled from Fullerton et al. 2006 and Mokiem et al. 2007). Note the large dispersion by nearly two orders of magnitude at fixed type. Crosses and an asterisks mark measurements from five bowshock-generating OB stars using the technique introduced in Kobulnicky et al. 2010 (hereafter K10) and described fully in Section 3. The new results follow the trend of published values, but the number of data points is small. The exceptional O4If star at the upper left lies above the mean trend for supergiants, but evolved stars are known to have especially large and erratic variations in their mass loss rates. We expect the bulk of targets to be late-O and early B stars where traditional methods become insensitive (see Section 3). With potentially ~100 well-studied, high-quality

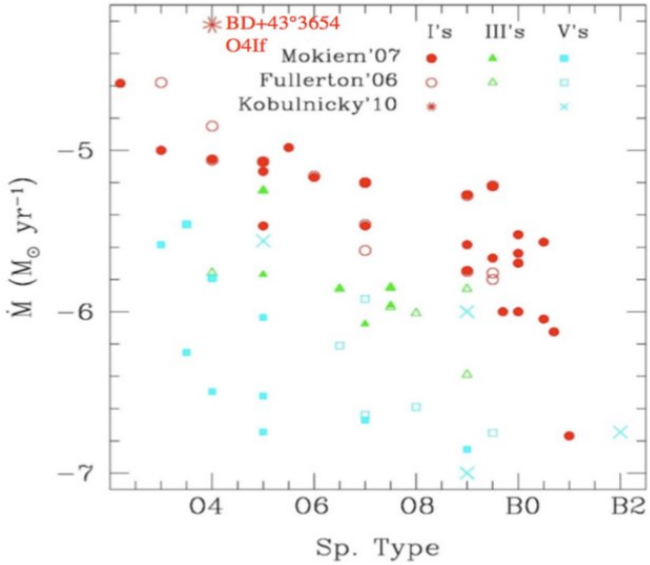

*Figure 2 — Mass loss rate in solar masses per year versus spectral type. Filled and open symbols show literature measurements, coded by luminosity class. The * and x's mark measurements of bowshock stars based on a subset of prototype objects from K10.*

bowshock objects to add to this diagram, we will significantly augment the body of measurements on mass loss rates *using a new technique grounded in a physically independent basis* from other methods. Even if the dispersions in $\dot{M}$ turn out to be substantial (as with current methods!), the large sample size will still permit a revealing comparison of the trends and zero point differences with respect to published samples. The present availability of large IR datasets in which hundreds of bowshock nebulae may be identified makes the moment ripe for a thorough vetting of this technique for $\dot{M}$ estimation to address a long-standing problem having far-ranging implications in fields as diverse as stellar evolution, stellar populations, supernovae, gamma-ray busts, and gravitational wave physics.

1.0 Scientific Justification

1.1 The Role of Massive Stars in Cosmic Evolution — Stars more massive than about 8 $M_\odot$ (B2V) end their lives in high-energy events — supernovae, hypernovae, and long-duration gamma-ray bursts (Woosley, Heger, & Weaver 2002). The ensuing luminous and mechanical energy sculpts the interstellar medium in galaxies, possibly triggers or terminates nearby star formation (Dale et al. 2005; Elmegreen 2011), expels hot hot gas from galaxies in high-velocity superwinds (Heckman, Armus, & Miley 1990; Veilleux, Cecil, & Bland-Hawthorne 2005), and spews fresh nucleosynthetic products into the cosmos (Woosley & Weaver 1995). The remnant neutron stars and black holes become dominant sources of X-ray emission in early-type and even in some young galaxies (Fabbiano 2006). Gravitational waves (GW) from such explosions, or from the compact remnants left behind, will be probed by the imminent generation of GW experiments such as LIGO and VIRGO (review by Fryer & New 2011). The possibility that very massive stars, M>150 $M_\odot$, form in the local universe (rather than just in the early universe at low metallicity; Crowther et al. 2010) has added a new dimension to the massive star odyssey. Even before their terminal explosive events, massive stars eject tens of solar masses of envelope material during main-sequence (MS), red- and blue-supergiant, luminous Blue Variable (LBV), and Wolf-Rayet (WR) stages of evolution. As such, massive stars are the dominant sources of ionizing photons, mechanical energy, and heavy elements in the universe. While the important role played by massive stars in cosmic evolution is well-established, the details regarding how they come to populate the various post-MS evolutionary channels are far from understood. Stellar mass loss remains prominent among the unsolved problems in stellar evolution.

1.2 Stellar Mass Loss — The fate of a massive star and its subsequent impact on its surroundings is ultimately dictated by the core mass at the end of nuclear burning, which in turn depends on the amount of mass lost through stellar winds during MS and post-MS evolution. Current scenarios predict that progenitor stars less massive than about 9 $M_\odot$ leave behind white dwarf remnants, stars from 9 to perhaps 25–40 $M_\odot$ produce neutron stars after exploding as a (H-rich) type IIp or IIL/b supernova. "Electron capture supernovae" are an especially interesting class of events originating in 10–12 $M_\odot$ stars (lower at lower metallicity) which produce massive ONe white dwarfs supported by electron degeneracy pressure; subsequent electron capture reduces this support, causing collapse to a neutron star and SN explosion (Iben & Renzini 1983; Poelarends et al. 2008). Given a typical IMF, this may be one of the most common SN mechanisms. Stars above about 40 $M_\odot$ form black holes following a (H-poor) type Ib/c supernova (Heger et al. 2003). Very massive stars above 100 $M_\odot$ may yield >100 $M_\odot$ black holes (Fryer & Kalogera 2001) that could form the seeds for the population of "intermediate-mass" black holes invoked to power super-Eddington X-ray sources in dense stellar clusters and nearby galaxies (Miller & Colbert 2004). *However, these limits are approximate in all cases and depend sensitively on assumptions about mass loss and stellar rotation.* Stellar rotation and mass loss are intertwined processes that jointly dictate stellar evolutionary paths (Meynet & Maeder 2000; Maeder & Meynet 2000); rapid rotation promotes mass loss through centrifugal forces or through ejection along the polar axis, while mass loss ultimately slows stellar rotation as angular momentum is conserved.

1.2.1 Mass Loss Theory—Puls, Vink, & Najarro (2008) reviewed the theoretical and observational status of attempts to predict and measure mass loss phenomena. The standard model of radiatively driven mass loss from hot stars (Lucy & Solomon 1970; Castor, Abbott, & Klein 1975) involves coupling the momentum of stellar photons to the photospheric plasma via absorption/scattering in resonance lines of abundant metal ions (C, N, O, Si) or low-lying states of Fe ions. Collisions of these atoms with the more abundant ions of H and He result in a net radial acceleration that can produce mass fluxes of several $x10^6$ $M_\odot$ yr^{-1}, significant enough to alter the mass of the star even on the short evolutionary timescales for massive stars. Radial flows begin near the stellar surface and reach terminal velocities, v_∞, up to several 1000 km/s at 10–15 stellar radii. Winds can even be driven from metal-poor stars via opacity in lines of H and He, albeit with much reduced efficiency. Thus, momentum in a stellar wind scales with the stellar luminosity, *L*, and a factor, *k*, that accounts for the number of spectral lines producing opacity in the atmosphere. When applied to millions of spectral lines tabulated in atomic databases and incorporated into models of stellar atmospheres, these principles result in a tight relation between the momentum of the stellar wind and the stellar luminosity – the wind momentum-luminosity relation (Puls et al. 1996).

Langer et al. (1994) proposed an evolutionary path for >60 $M_\odot$ stars in which they proceed through a sequence of spectroscopic stellar types from O -> Of -> H-rich Wolf-Rayet (WN subtype) -> LBV -> H-free WR (WN subtype) -> Wolf-Rayet (WC subtype) -> supernova. Stars in the 8–40 $M_\odot$ range may instead transition through red and blue supergiant phases before the final supernova. Mass loss rates vary dramatically along this path, at times driven by stellar pulsational instabilities, peaking at $\dot{M}$ = $5x10^{-3}$ $M_\odot$ yr^{-1} during the LBV eruptions. Less massive stars are predicted to have rates of $1x10^{-9}$ $M_\odot$ yr^{-1} or even smaller while on the main sequence. Variations in stellar luminosity and atmospheric opacity during the lifetime of a star lead to highly variable $\dot{M}$. Additional complications arise from critical transitions in the ionization state of an atmosphere that depend sensitively on temperature and composition. As the effective temperatures drops below ~25,000 K the dominant source of opacity suddenly shifts from Fe IV to Fe III, leading to increased opacity and larger mass loss rates over a small range in temperature (Lamers et al. 1995; Vink et al. 1999). This "bi-stability" mechanism is one example of phenomena that complicate $\dot{M}$ predictions. Additional effects resulting from stellar rotation, non-sphericity, wind-compressed equatorial disks (Bjorkman & Cassinelli 1993), and magnetic activity are not yet convincingly modeled. A full theoretical description of mass loss is still a work in progress.

1.2.2 Mass Loss Observations — Measurements of $\dot{M}$ for massive stars align around three main techniques, all of which involve measuring a density tracer at some location in the wind and then applying a velocity field prescription to compute a mass flux. All of these approaches, as highlighted in Puls, Vink, & Najarro (2008), involve fitting spectra or SEDs to atmospheric models coupled with radiative transfer calculations using a particular analytic parameterization of the velocity and density structure of the wind, v(r) and ρ(r), respectively. Hence, "observed" mass loss rates rest upon a foundation of theoretical modeling involving assumptions that can vary drastically from one object to another or one method to another. $\dot{M}$ measurements grounded in NLTE atmosphere models and models including effects of non-sphericity, shocks, and clunps/inhomogeneities in winds have only recently been attempted (Muijres et al. 2011). Nevertheless, the predicted and "observed" mass loss rates at least seem to scale with luminosity and stellar mass in the expected manner, so some self-consistency is achieved.

UV P Cygni profiles — UV absorption lines of C IV, N V, Si VI, P V are produced in the blue-shifted wings of P Cygni profiles in hot, mass-losing stars. These lines are fit with models to infer $\dot{M}$ (e.g., Garmany et al. 1981; Pauldrach et al. 2004). These resonance lines are often opaque, rendering them unreliable, but some non-saturated instances have been exploited (Howarth & Prinja 1989). However, even these always appear to be optically thick at some local locations/velocities in the wind. This

signature is ostensibly a consequence of localized clumps of high density material, but the magnitude of effects due to clumps/inhomogeneities in the wind are not yet resolved (Owocki & Puls 1999).

Hα measurements — Recombination of H^+ in the stellar wind produces an Hα emission line that is thought to be optically thin and useful for inferring the total mass in the wind given the operational ease of acquiring ground-based optical spectra. Klein & Castor (1978), Leitherer (1988), Puls et al. (1996), Markova et al. (2004), Markova & Puls (2008) and others have utilized Hα spectroscopy to derive mass loss for large samples of Galactic stars. These analyses compare Hα profiles to stellar atmosphere and wind models to again derive a velocity field and density structure. Most problematic in this approach is that the Hα emissivity is proportional to density squared, n^2, so that clumps/inhomogeneities in the wind, introduce large degeneracies in the best fit model parameters, and hence, in the $\dot{M}$ determinations. In "The Discordance of Mass-Loss Estimates for Galactic O-Type Stars" Fullerton, Massa, & Prinja (2006) compared UV P^{+4} -derived mass loss rates to those from Hα and concluded that clumping results in $\dot{M}$ being overestimated by factors factors of as much as 130 when using Hα! Models attempting to reconcile observed and theoretical rates depend sensitively on the clumping factors and porosity of the wind, so discrepancies remain, ranging from factors of 10–100 (Muijres et al. 2011).

Radio continuum — Free-free emission in expanding ionized winds may be observed as a radio continuum or infrared excess. This excess, again when coupled with a model for the velocity and density structure of the wind, has been used to infer a mass flux (Abbott et al. 1980, 1981; Lamers & Leitherer 1993). While radio and Hα results appear to agree with each other, free-free processes again depends on n^2, and the pernicious clumping effects in winds again cast doubt on the reliability of the results.

Puls, Vink, & Najarro (2008) conclude that, while substantial progress has been made to understand mass loss phenomenae, there remain considerable discrepancies between theory and observations, and consequently, uncertainties on the actual mass loss rates may amount to factors of 10 to 100. In addition to the unsolved problem of clumping, models still fail to provide enough momentum to match observations for stars with weak winds, i.e., later than about O7V a discrepancy known as the "weak wind problem" (Muijres et al. 2012; Puls et al. 1996). Given the importance of mass loss on stellar and thereby cosmic evolution, the magnitude of current gaps in our understanding make this topic an area of critical concern for a wide range of astrophysical sub-disciplines.

2.0 Runaway Stars and their Bowshocks as Laboratories for Mass Loss

2.1 Runaway Stars—A noteworthy fraction of massive stars appear surprisingly far from the molecular clouds and H II regions where they are born, both in the Milky Way (Tobin & Kilkenney 1981; Keenan & Dufton 1983) and in external galaxies (e.g., Wilson 1991). Maxwellian velocity dispersions typical of massive clusters (~10 km/s) dictate that OB stars should wander no farther than ~100 pc during their 10^7 yr lifetimes. Blaauw & Morgan (1954) first identified a population of stars having space velocities >40 km/s, later termed "runaways" (Blaauw 1961). Gies & Bolton (1986) found that 10–25% of O stars are runaways having space velocities exceeding 30 km/s, the current nominal threshold for identification as such. These may be either ejected from binary systems as a result of asymmetric supernova explosions (Blaauw 1964; Fryer, Burrows & Benz 1998) or accelerated by dynamical interactions in small stellar clusters during close 3- or 4-body encounters (Heggie 1975; Hut 1984; Gies 1987; Leonard & Duncan 1990). Runaway OB stars are likely to be responsible for producing the halo population of pulsars (Gvaramadze et al. 2009; Rutledge et al. 2008), some extragalactic supernovae and gamma-ray bursts, and possibly some *Fermi* gamma-ray sources (del Valle, Romero, & De Becker 2013). While some runaways are recognized by their large proper motions or radial velocities, a growing class have been identified by the presence of a distinctive "bowshock" nebula that precedes a star in supersonic motion.

2.2 Stellar Bowshocks from Runaway Stars—Arc-like features flanking high-velocity stars were identified in optical emission lines (Gull & Sofia 1979) and in IRAS infrared images (van Buren & McCray 1988). These were interpreted as shocks driven into the interstellar medium by massive star winds. IRAS surveys revealed bowshock candidates, including the cometary class of compact HII regions which were modeled as bowshocks (van Buren et al. 1990). With the proliferation of sky surveys, particularly spacecraft mission in the infrared (MSX, ISO, Akari, *Spitzer,* WISE*)* bowshocks have become a well-established class of objects with dozens of candidates reported (Noriega-Crespo, van Buren, & Dgani 1997; Comeron & Pasquali 2007; Povich et al. 2008; Gvaramadze & Bomans 2008; Gvaramadze et al. 2011; Kobulnicky et al. 2010, 2012). **Figure 1** (page 1) shows three examples from the Kobulnicky et al. (2010) *Spitzer* survey of the Cygnus X complex, with red/green/blue depicting the *Spitzer* IRAC 4.5/8.0/24 μm bands, respectively. The powering early-type star is visible at the shortest wavelengths, located along the axis of symmetry near the apsis of the nebula. In the left panel, the exciting B0.2III star has a measured proper motion in the direction of the yellow vector and lies displaced from the symmetry axis. Bowshocks may also be formed by a flow of hot gas around a stationary star, such as in champagne flows around the peripheries of M17 and the Carina Nebula (Povich et al. 2008; Smith et al. 2010; Sexton et al. 2013). Either way, the physics of the bowshock formation resulting from the relative velocities between a star and the ambient ISM remain the same.

Wilkin (1996) developed an exact analytical formalism to describe stellar wind bowshocks, building upon the more general case of interstellar bubbles (Weaver et al. 1977) and early work on the solar wind bowshock (Baranov, Krasnobaev, & Kulikovski 1971). Wilkin (2000) extended the treatment to non-axisymmetric bowshocks produced in the presence of density gradients in the surrounding ISM. Comeron & Kaper (1998) and van Marle et al. (2011) performed numerical simulations of bowshocks preceding massive stars under more complex ISM geometries and showed that a diversity of morphologies, including asymmetry, could result.

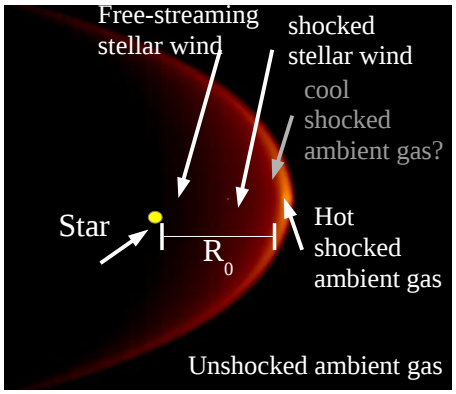

Figure 3 — Analytic/numerical bowshock appearance for star motion transverse to the line of sight, with key physical features labeled.

A bowshock forms at a distance, R_0, ahead of the star, dictated by the point where momentum flux (i.e., pressure) of the stellar wind balances that of the ambient ISM in the reference frame moving with the star. R_0 is known as the "standoff distance," depicted in **Figure 3**, with notation of Comeron & Kaper (1998) and Wilkin (1996). The standoff distance is derived by equating the ram pressure from a stellar wind of density ρ_w and velocity v_w with ram pressure supplied by the ambient ISM of density ρ_a moving at velocity v_a in the frame of the star

$$\rho_w v_w^2 = \rho_a v_a^2 \quad . \qquad (1)$$

The density of an expanding stellar wind, in terms of the mass loss rate, $\dot{M}$, and distance from the star, r, is

$$\rho_w = \frac{\dot{M}_w}{4\pi r^2 v_w} \quad , \qquad (2)$$

and r becomes R_0, the standoff distance where the wind and ISM are in pressure equilibrium. It follows that the standoff distance is

$$R_0 = \sqrt{\frac{v_w \dot{M}_w}{4\pi \rho_a v_a^2}} \quad . \qquad (3)$$

K10 proposed inverting this expression to solve for the wind mass loss rate in terms of observables,

$$\dot{M} = \frac{4\pi R_0^2 \rho_a v_a^2}{v_w} \quad . \qquad (4)$$

The mass density ρ_a can be replaced by μn_a, where the mean mass per H atom is $\mu = 2.36 \times 10^{-24}$ g and n_a is the standard ambient number density in cm^{-3}. When reduced to convenient astrophysical units, this can be expressed by a slightly revised form following Povich et al. (2008) and K10,

$$\dot{M}\left(solar\ masses\ yr^{-1}\right) = 0.4\,\frac{\left[R_0(pc)\right]^2\left[v_a\left(km\,s^{-1}\right)\right]^2 n_a\left(cm^{-3}\right)}{v_w\left(km\,s^{-1}\right)} \quad , \qquad (5)$$

where the coefficient 0.4 could be as large as 0.8 if the dominant gas-phase species were molecular instead of atomic. The quantities on the right-hand side are, in principle, directly observable. The next section describes a methodology for measuring these parameters in a large sample of OB bowshock stars.

3.0 Proposed Research Program

We propose to enlist the aid of several thousand citizen scientists worldwide to examine infrared mosaics, conduct a comprehensive survey for bowshock nebulae, and exploit their unique physics as a new window into the the mass loss rates. We expect to find hundreds of bowshock candidates throughout the Galactic Plane, making the numbers of objects comparable to the samples analyzed using Hα, radio, or UV techniques. While we expect that the canonical mass loss indicators will continue to be improved as efforts to understand wind clumping are more fully developed, *the recent completion of several wide-area IR surveys provides a ripe opportunity to address a critical issue in stellar and cosmic evolution using a physically independent approach*. Even if we reasonably anticipate that there will be unavoidable systematic effects resulting from our choice of dust models or calculated ambient ISM densities, these are at least a *different* set of biases than those inherent in the existing body of measurements which rely on the same set of stellar atmosphere and wind velocity prescriptions.

3.1 Identifying a Large Sample of Milky Way Bowshocks—Obtaining a statistically meaningful set of mass loss measurements requires large sample of stars producing bowshocks. There are already several dozen known examples in the literature (see references in Section 3.2 above), selected morphologically from infrared surveys with IRAS, MSX, *Spitzer*, and WISE. Bowshocks identified with IRAS (Noriega-Crespo, van Buren, & Dgani 1997) are the largest, a result of the large IRAS beamsize, and also have the highest surface brightness, but the sample size is quite small. This sample is likely already complete. The MSX mission provided considerable improvement in sensitivity and beamsize, resulting in additional detections (e.g., Comeron & Pasquali 2007). A few have been detected at Hα, but the high opacity at optical wavelengths relative to the mid-IR ($A_{H\alpha}/A_{L'} \approx 9$) make infrared searches a far superior technique.

Survey	Beam	Bandpasses	Sensitivity (point src.)	Coverage
WISE	6" - 12"	3.4, 4.6, 12, 22 μm	0.068 0.098, 0.86, 5.4 mJy	All sky, but |b|<20° used
Spitzer GLIMPSE + MIPSGAL and related surveys	2.4" - 6"	3.6, 4.5, 5.8, 8.0 /24 / 70 μm	variable; 0.015, 0.02 mJy for Gl360 and DEEP GLIMPSE; factor of 4-8 higher for GLIMPSE I,II,3D	Galactic Plane |b|< ~1° + additional regions; ~1000 sq. deg. total including SMOG, Cygnus-X, Vela surveys

3.1.1 Bowshocks in Publicly-Available Imaging Data—Table 1 summarizes the key parameters for datasets comprising the backbone of our search effort. The completion of the WISE all-sky survey and the Spitzer GLIMPSE legacy programs (see Kobulnicky et al. 2013 for a summary table on the various incarnations of the GLIMPSE programs) provide the advances in sensitivity and sky coverage that enable this program on a large scale. These spacecraft surveys generated wide-area, multi-band infrared datasets that are now publicly available in large mosaic formats.

K10 used a portion of the *Spitzer* Cygnus-X legacy survey (Hora et al. 2008, Beerer et al. 2010) to identify ten probable bowshock objects. The Cygnus-X region boasts a rich population of massive stars where bowshocks and runaway stars appear abundant. Our visual search technique will use a similar approach, but harnessing the power of ***Zooniverse*** citizen science to examine ~14,000 square degrees of sky. Many objects exhibit morphologies similar to partial arcs or rings, so culling the list to retain high-confidence candidates requires that an object meet several criteria:

1. A nebular non-circular arc or partial arc present in at least one of the WISE (12 or 22 μm) or Spitzer (8.0 or 24 μm) bands; K10 noted that some bowshocks appeared prominently at 24 μm band but not at the shorter bands where poly-cyclic aromatic hydrocarbon (PAH) emission is strong; conversely, a few bowshocks were best seen at the *Spitzer* IRAC 3.6 and 5.8 bands, and likely contain PAHs. Sexton et al. (2013) find that colors of bowshocks are distinct from PAH-dominated nebular sources.

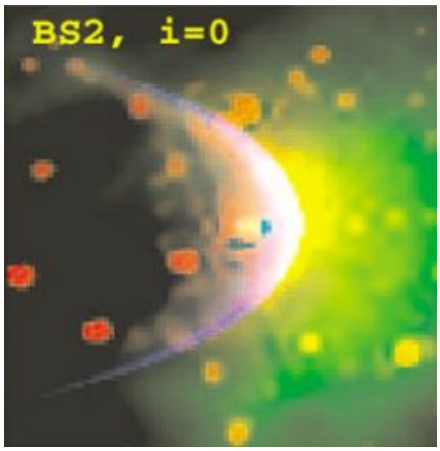

Figure 4 — Theoretical bowshock shape (blue) compared to Spitzer 8 (green) and 24 μm (red) morphology, from K10.

2. A point source located along the axis of symmetry of the nebula near the apsis; these are best seen at 3.4 or 4.5 μm where the extinction is a minimum and the stellar photospheric fluxes are still relatively high. Deep near-IR data (e.g., UKIDSS JHK) will also be used, where available.
3. Intrinsic colors consistent with an O or early B type star. The (*H*-4.5 um) color (or 3.6-4.5 um color) is an effective indicator of interstellar reddening, so that an intrinsic color can be recovered by the Rayleigh-Jeans color excess method (Majewski, Zasowski, & Nidever 2011).
4. Morphology similar to the theoretical distinctive bowshock shape, as pictured in **Figures 3 and 4** for an inclination of 0°.

Bowshocks can be identified as such only if inclinations are less than about 30°, requiring the star's velocity vector to lie near the plane of the sky. This is statistically more likely than a predominantly radial velocity vector, given the ratios of solid angles subtended by transverse versus radial motions (e.g., Harwitt, ch. 4.1). Based on our experience with visual examination of the 24 sq. degree Cygnus-X region, we plan to conduct a visual examination of all ~14,000 square degrees at $|b| < 20°$ using mosaics from the *Spitzer* and WISE image atlas. Confining the search for bowshocks to within 20°of the Plane will encompass all of the major massive star regions and the areas most likely to exhibit bowshocks from OB stars.

3.1.2 ***Zooniverse*** *Citizen Science*—Co-PI Povich is a founding team member and principal architect of the Milky Way Project (MWP), part of the ***Zooniverse*** suite of online Citizen Science projects (Lintott et al., 2008). Zooniverse has built a global network of >500, 000 volunteers who, via the internet, collaborate with professional scientists and contribute to discoveries at the frontiers. We will use the established MWP citizen science apparatus to harness the power of thousands of volunteers from around the world to identify bowshocks in infrared survey images. The MWP grew out of previous findings by the GLIMPSE team that Galactic H II regions present "bubble-like" morphology in IR images (Povich et al., 2007; Watson et al., 2008) and that, as in the case of bowshocks, visual inspection provides the most efficient means of identification. The MWP found thousands of interstellar bubbles from over 1 million candidates identified amidst the complex, structured nebular emission in the Galactic Plane.

Co-PI Povich has developed software to prepare 3-color, square-root-stretched images from *Spitzer* mosaics for examination by the public. The images created for the MWP bubbles searches thus far come

in two different combinations, 4.5/8.0/24 μm and 3.6/4.5/8 μm. The former will be used to find 24 μm bowshocks, while 8 μm bowshocks stand out better in the latter. To extend coverage to $|b| < 20°$ we will adapt our image-generating software to ingest *WISE* atlas images and output color composites combining 4.6/12/22 μm and 3.5/4.6/12 μm, which will highlight the same structures as our existing *Spitzer* images.

We expect to locate ~300 high-confidence bowshock candidates based on a rough scaling of bowshock source densities in a few existing searches (e.g., ten in Cygnus-X by K10; eight in the Carina Nebula region by Smith et al. 2010 and Sexton et al. 2013; seven near NGC 6357 by Gvaramadze et al. 2011). The density of complex, confusing diffuse structures is higher near the Plane, so that the search will become less confused at higher latitudes (see GLIMPSE mosaics). The superior angular resolution of *Spitzer* (where available) relative to WISE is critical to bowshock identification where the nebulae are small and the powering star has a small angular separation from the nebula. For example, the second panel of Figure 1 shows a *Spitzer*-identified bowshock where the standoff distance is only a few arcsec and the angular width of the bowshock is only 10 arcsec. Although the resulting catalog of bowshocks will not be "complete" in any rigorous sense, (sources with unfavorable projections or those that lie in high diffuse background areas will be missed) it will comprise the largest list of uniformly selected targets that will be achievable with the current suite of infrared surveys anytime in the foreseeable future.

3.2 Measuring Key Bowshock Parameters—Equation (5) expresses the stellar mass loss rate in terms of the standoff distance R_0, the stellar space velocity relative to the ambient ISM, V_a, the ambient ISM density n_a, and the stellar wind velocity, V_w. All of these quantities are, by various methods, measurable.

3.2.1 Standoff Distances, R_0—**Figures 3 & 4** illustrate how the distance from the star to the bowshock apsis can be measured from infrared images by inspection, modulo a factor *sin i*, the correction for the (unknown) projection, if the distance to the star is known. The projection factor *sin i* will be assumed to be unity, given that only objects with $i \approx 0° - 30°$ will be observed as bowshocks. The standoff distance is then $R_0 = D\varphi$ where D is the distance to the target and φ the angle from star to bowshock apsis.

Distances, D, will be determined in several ways. For bowshocks affiliated with a well-studied star clusters such as Cygnus OB2, Carina, or NGC 6357 we will adopt accepted literature distances obtained through main sequence fitting, spectroscopic parallax, or kinematic distances. An increasing number of prominent star forming regions, where runaway OB stars are likely to be most concentrated, have trigonometric distances from VLBA maser parallaxes (e.g., Rygl et al. 2012; Xu et al. 2011). We expect the majority of bowshocks to be located near such large star forming regions where massive stars are abundant. In other cases bowshocks can be linked to specific clouds seen in molecular line surveys such as the public ^{13}CO Galactic Ring Survey (Jackson et al. 2006) where kinematic distances can be obtained from radial velocities. For seemingly isolated bowshocks lacking published spectra, such as the one powering IRAS 03063+5735 in the outer Galaxy (Kobulnicky et al. 2012), we will obtain our own optical spectra using the University of Wyoming 2.3 m telescope (WIRO) and longslit spectrograph. The PI has abundant access to WIRO at the level of >90 nights per year. Even if we require followup for as many as ~200 new bowshock stars accessible from the north (about 70% of the Galactic Plane), classification spectra could be done at a rate of 5-8 per night (targets are likely to be V=13–17 from prior samples, a result of significant extinction), requiring perhaps 30 nights of observing. Experience gained during prior optical spectroscopic programs on massive stars means that we have a streamlined data reduction and analysis procedure already in place (e.g., K10; Kobulnicky et al. 2012, Kiminki et al. 2007; Kiminki & Kobulnicky 2012). Additional spectra of southern (mainly 4th quadrant) targets inaccessible from WIRO would be attempted through additional southern telescope proposals or service time.

Figure 5 shows an example spectrum (upper) of the B0.5Ib star in the first panel of **Figure 1**, with labels marking key diagnostics of temperature and luminosity class. Kobulnicky et al. (2012) presented a series of helium line ratio diagnostics for measuring effective temperatures for hot stars from He II 5410 Å and He I 5876 Å. The indices are calibrated against current atmosphere models of hot stars including TLUSTY (Lanz & Hubeny 2003) and CMFGEN (Hillier & Miller 1998) shown to faithfully reproduce observed spectra (Massey et al. 2013). Armed with spectral type and luminosity classifications, we will determine spectrophotometric distances from the distance modulus, in the usual manner, including effects of extinction, A_V. We have developed a generalized software tool to fit broadband stellar SEDs to Castelli & Kurucz (2004) model atmospheres reddened either by Cardelli, Clayton, Mathis (1989) or Fitzpatrick & Massa (2007) reddening curves with A_V and R_V as free parameters, where the ratio of total to selective extinction is $R_V = A_V / E(B-V)$. Allowing for a variable R_V is necessary because, as shown by Vargas-Alvarez et al. (2013), the distance to the Galactic open cluster Westerlund 2 changes from ~8 kpc to ~4 kpc when R_V is measured to be 3.8 instead of assumed to be the canonical mean interstellar value of 3.1. We will use 2MASS JHK photometry along with public multi-band optical Tycho-2, USNO-B2/NOMAD, DSS, IPHAS, and other published sources of broadband photometry on stars we expect to range in magnitude from V=10–18 for O and early B stars at 1–5 kpc distances with extinctions A_V =2 to ~8 mag. The impact of R_V variations will be minimized by using spectral typing to assign temperatures and then obtaining luminosities via fitting the IR SEDs in lieu of using visual-light magnitudes (Povich et al. 2011). The incidence of binarity, although high among OB stars in general (Kiminki & Kobulnicky 2012; Sana et al. 2012), is low among runaways (Gies 1987). This removes contamination from close companions as a complicating factor in computing distances for runaways. Furthermore, the selection of preferentially single stars as targets simplifies the interpretation by removing potential effects of companion interactions that have been invoked to drive mass loss, especially during post-MS evolution (e.g., Smith et al. 2011). Finally, the first releases of ***Gaia*** parallaxes are anticipated by 2017, in time for use in the final stages of this program.

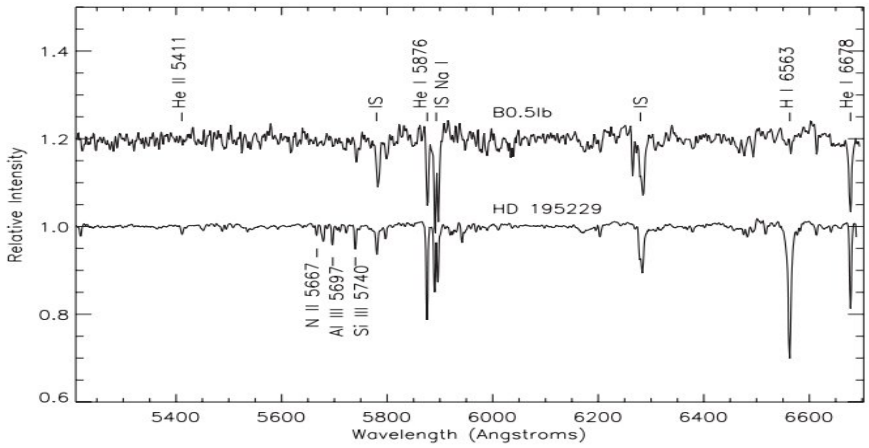

Figure 5 — Optical spectrum of a bowshock #3 (upper) from K10 obtained at the Wyoming Infrared Observatory. Analysis of helium and other line ratios and comparison to standard (lower) stellar atlas spectra classify this bowshock star as B0.5Ib.

R₀ Summary: Although $\dot{M}$ scales as R_0^2, and $R_0 \propto D$, we expect that distances will be known to 25% in most cases so that the distance errors affect the final mass loss rates at a minor level. For typical standoff distances of R_0=0.05 to ~1 pc represent wind expansion timescales of tens to hundreds of years, meaning that we would measure mass loss rates averaged over these kinds of intervals. On such temporal and spatial scales, effects of $\dot{M}$ variations and clumping that plague measurements on few stellar radii scales may be significantly ameliorated, especially if clumps are destroyed in shocks (Pittard 2007).

3.2.2 RelativeVelocities, V_a—The relative velocity between a star and the ambient medium, V_A, for a star traveling at supersonic speeds will be near the canonical runaway speed of ~25 km s^{-1} (Stone 1981; Gies 1987). This is several times the velocity dispersion of OB associations and highly supersonic compared to the sound speeds $c_s = \sqrt{\gamma P/\rho}$ < 10 km s^{-1} for the cool neutral or warm ionized ISM phases. Runaway velocities much greater than 25 km s^{-1} have been documented (e.g., Heber et al. 2008), but are statistically unlikely from Maxwellian arguments. Adopting V_A=25 km s^{-1} is a reasonable starting point and likely correct within a factor of ~2 even in cases where the relative velocity is the result of an HII region flow (~10 km/s) impinging upon a quasi-stationary star.

We will use proper motion data from Hipparcos (Perryman et al. 1997) and the USNO UCAC 2 to measure proper motions for stars sufficiently bright and with sufficiently high space velocities to be reliably detected. This corresponds to stars brighter than about V=12 mag and proper motions μ> ~2 mas yr^{-1} for HIPPARCOS and R<16 mag, μ >2–6 mas yr^{-1} for the UCAC2. For example, a runaway with V=60 km s^{-1} transverse motion would have μ=12 mas yr^{-1} at 1 kpc distance. Stars with exceptional space velocities can be identified and measured at the level of factors of 2 or better required for our purposes. Again, proper motions may be available from Gaia in time for the final stages of this effort.

Although we expect the radial velocities of bowshock stars to be unremarkable in most cases, our optical spectra from WIRO described above can be used to determine the line-of-sight components to a level of 3–8 km s^{-1} based on our experience using the same spectroscopic configuration as OB stars in Cygnus OB2 (e.g., K10; Kobulnicky et al. 2012; Kiminki et al. 2007; Kiminki & Kobulnicky 2012). These data, furthermore, would let us identify rare runaway binary systems (Gies 1987; Perets 2009). The existence of such systems supports that idea that some runaways are formed in N-body encounters, and improving the statistics of such objects will help refine the scenarios that may produce them.

<u>V_a Summary</u>: Stellar velocities can be assumed to be, within a factor of two, ~30 km s^{-1} relative to the ISM, and exceptionally large velocities should have measurable proper motions from which velocities may be measured. Although $\dot{M} \propto V_a^2$, the range in V_a is small compared to the magnitude of the wind mass loss discrepancies that exist. For a suitably large sample of stars our nominal value is adequate for obtaining mean mass loss values as a function of spectral type.

3.2.3 Stellar Wind Velocities, V_w—Terminal wind velocities ($V_\infty \cong V_w$) have been extensively documented using the blue-shifted wings of P Cygni UV absorption profiles in the context of measuring stellar mass loss (e.g.,Prinja, Barlow, & Howarth 1990; Lamers, Snow, & Lindholm 1995; Martins et al. 2005; Crowther, Lennon, & Walborn 2006). These velocities are generally straightforward to measure and uncontroversial. They range from 400 – 1900 km s^{-1} for late O to B3 supergiants and between 3000 – 500 km s^{-1} for O3V through ~B2V stars. Measurements have been tabulated as a function of spectral type and luminosity class by numerous authors, and we will adopt the appropriate average V_∞ for our targets once spectral types are known fro mour WIRO spectroscopic campaign. For those few targets accessible to HST+COS, we would propose measurements of V_w separately.

<u>V_w Summary</u>: Terminal velocities are not significantly in dispute, so values may be adopted from published works with minimal impact on science goals since $\dot{M} \propto V_w^{-1}$.

3.2.4 Ambient ISM Densities, n_a—The final and most challenging observable is the ambient interstellar density. Our prescription for n_a involves performing photometry using irregular bow-shock shaped apertures on the *Spitzer*/WISE images at 3.6, 4.5, 5.8, 8.0, 22/24 and 70 microns, as available in public archives. *Spitzer* MIPS 70 μm data would be supplemented by *Herschel* 70 μm data (~6" FWHM beam),

where possible, from the Hi-GAL survey (Molinari et al. 2010) covering the inner 120 degrees of the Milky Way to b=±1°. Given knowledge of the distance, the infrared flux SED can be turned into an infrared luminosity SED. Angular size can be turned into a volume using the adopted distance.

The luminosity and volume of a nebula then lead to an estimate of the number density by fitting the SEDs to models of interstellar grain emissivity. We adopt Li & Draine (2001) dust models, updated Draine & Li (2007), to fit the infrared SEDs of astrophysical dust based on *Spitzer* observations in both Galactic and extra-galactic contexts. The models are described by three free parameters:

1) q_{PAH}: the fraction of PAH molecules, by mass. $0.47\% < q_{PAH} < 4.58\%$ in 7 bins;

2) U_{min}: the minimum interstellar radiation field to which the dust is exposed, in terms of the mean interstellar radiation field, U_{ISRF}, of Mathis, Mezger, & Panagia (1983), 2.3×10^{-2} erg s^{-1} cm^{-2}. $0.1\ U_{ISRF} < U_{min} < 25.0\ U_{ISRF}$ in 23 bins;

3) U_{max}: The maximum interstellar radiation field in 5 bins from $10^3\ U_{ISRF}$ to $10^7\ U_{ISRF}$.

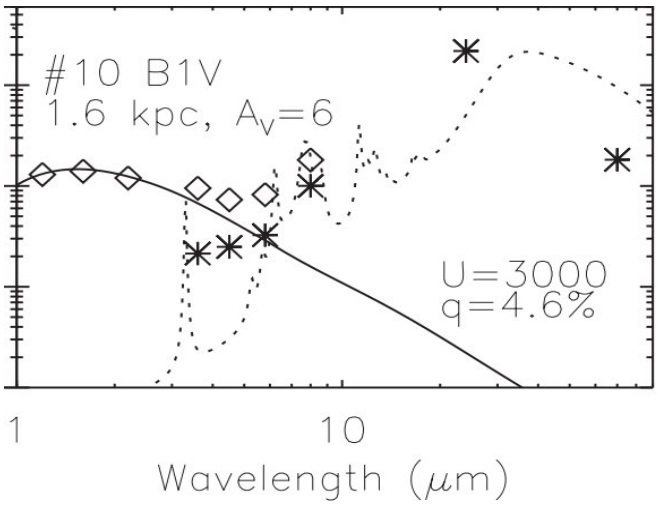

Figure 6 — Representative spectral energy distribution of a bowshock-producing star (♦'s) and the bowshock ISM material ('s) extending from 2MASS 1.2 microns through Spitzer 70 micron measurements. The solid curve shows a reddened stellar photosphere of the appropriate spectral type and distance. The dashed line plots a Draine & Li (2007) dust model for ionization parameter U=3000 and PAH fraction q=4.6%.*

Figure 6 shows an example of fitting Draine & Li (2007) dust models to one of the bowshock nebulae from K10. Diamonds mark the stellar flux, from 2MASS JHK photometry through *Spitzer* IRAC bands [3.6]–[8.0] μm. Asterisks denote bowshock measurements from 3.6 to 70 μm. The solid line is the reddened stellar SED while the dashed line is the dust model. The slope of the 24 to 70 μm SED is sensitive to U while the 5.8 and 8.0 μm points are sensitive to PAH fraction. Fitting was done by eye in K10 , but we will develop an automated least squares routine for bowshock nebulae to be run by undergraduate research assistants as part of this effort. K10 assumed that $U_{min}=U_{max}$, but we will generalize our code to allow a range of limits. In practice, the radiation field illuminating the surrounding nebulae is likely to be dominated by the OB star, so that the radiation field may be estimated from the stellar temperature, T_{eff}, the stellar radius, R_*, and the standoff distance, R_0,

$$U = \frac{R_*^2 \sigma T_{eff}^4}{R_0^2} \quad , \tag{6}$$

where σ is the usual Steffan-Boltzmann constant. Indeed, K10 found good agreement between U estimated from the slope of the IR SED and that estimated from Equation 6. Draine & Li (2007) tabulated the emissivity ε in erg s^{-1} per hydrogen atom as a function of wavelength for each model. The number density becomes

$$n_a = \frac{F\, 4\pi D^2}{\epsilon V} \quad , \tag{7}$$

where F is the measured flux, D the distance to the star, and V the volume of the emitting region. K10 used rough emitting volumes characterized as hollow cones. Typical number densities were ~100 cm^{-3} from the K10 sample, but may be in the range 1--10 for the diffuse ISM. Assumption of a constant

density over the nebulae is almost certainly too simplistic. Often, bowshocks are observed as bright nebulae where a star is encountering a molecular cloud (e.g., #2 from K10). As part of our effort we would improve upon uniform density assumptions by using the theoretical bowshock profile rotated about the symmetry axis to produce more reliable volumes. Ambient densities will also be computed over localized volumes, even on a pixel-by-pixel basis, near the bowshock apsis and compared to global average results to understand the impact of density inhomogeneities. In K10 we accounted for differences in the pre-shock versus post-shock density (factors of ~4) by applying a correction factor of two, allowing for the possibility that dust and PAHs are destroyed in shocks. Background diffuse would be subtracted using a 2D sky estimating routine, and unrelated point sources would be subtracted prior to photometry to produce improved fluxes and SEDs.

n_a *Summary*: Because $V \propto D^3$, the uncertainties on n_a scale as D^{-1}, linearly with F which scales as D^{-2} , and as ε^{-1}. Since $\dot{M}$ is $\propto n_a$, estimates of ambient density affects the mass loss rate proportionally.

4.0 Workplan and Personnel

The work would be conducted one full-time graduate student and several undergraduates at UW and Cal Poly Pomona supervised by the Co-PIs. The PI and Co-PI are senior members of the *Spitzer* GLIMPSE legacy teams and is intimately familiar with the *Spitser and WISE* image and photometry datasets required. Key milestones and deliverables include:

- 2015 fall-winter: Visit by UW workers to Cal Poly Pomona for project launch meeting. Assembly of WISE & *Spitzer* image mosaics from public databases; creation of 3-color mosaics imported to ***Zooniverse***; initial visual searches for bowshock candidates; collection of literature bowshock candidates and their associated data; Launch of ***Zooniverse*** portal. Implementation of ***Zooniverse*** in Astro 101 authentic investigation course module at Cal Poly, and annually.
- 2015 spring-summer: Acquisition of optical spectra from WIRO on selected targets; analysis and compilation of distances & spectral types; start of IRAF/IDL procedures for photometry of bowshock nebulae; write proposals for southern telescope time, if required; Cal Poly Pomona students & faculty visit to Wyoming for observing and data analysis.
- 2016 fall-winter: preparation of *Paper I: "An All-Sky Sample of Stellar Bowshocks from Runaway Stars"*, listing targets, spectral types, and probable distances; assembly of stellar SEDs for bowshock targets from published optical and IR surveys; observe southern targets, if required; presentation of results at AAS or similar meeting; Wyoming student & faculty visit to Cal Poly Pomona.
- 2016 spring-summer: Completion of IDL code for bowshock photometry; start of IDL code for fitting bowshock SEDs to dust models; start of photometry of bowshock sample using WISE+Spitzer images; derivation of extinctions for bowshock stars through broadband SEDs; reduction of southern target optical spectra, as required. Cal Poly Pomona students & faculty visit to Wyoming.
- 2017 fall-winter: Completion of bowshock photometry and fitting of dust SEDs; completion of extinction and dereddening of bowshock stars; assembly of final set of stellar types, extinctions, distances, standoff distances, wind velocities, and ISM densities required for mass loss computation; presentation of results at AAS or similar meeting.
- 2017 spring-summer: Calculation of mass loss rates & comparison to literature values; Completion of *Paper II: "Mass Loss rates for OB Runaway Stars".* Presentation of results at an international conference, such as the *Massive Stars* series of IAU meetings.

5.0 Broader Impacts

Our program will develop a new branch of the Milky Way Project (MWP), one of the time-tested ***Zooniverse*** citizen science programs, involving thousands of people worldwide in the enormous task of cataloging bowshock nebulae. MWP volunteers numbered >15,000 from 175 countries! Since its launch in December 2010, the MWP has been one of the Zooniverse's most important projects. The MWP received approximately 4 years worth of human attention from volunteers in the past year, making it the 5th most intensive Zooniverse project out of 18 live during that time. The MWP has proven that citizen scientists can move beyond answering basic questions about astronomical data to investigate and make discoveries under the guidance of professional scientists. They continue to show enthusiasm for the project, and thousands of people visit the site every week. The *WISE* images processed for the MWP will have broad citizen science utility beyond searching for bowshocks, as they can also be used to search for IR bubbles, protostellar jets, star clusters, and galaxies in the Zone of Avoidance, potentially spawning a host of new citizen science investigations.

By establishing a California–Wyoming Astronomy Research Exchange (C–WARE), our program will provide several graduate and undergraduate students at each institutions with hands-on experience in astronomical observing and data reduction at the WIRO telescope where observers to everything from fill the Dewar and set the grating angle to troubleshoot problems. This kind of practical training is becoming increasingly rare in our age of remote and archive-only astronomical science, and it will be a uniquely valuable experience for students from Cal Poly Pomona, a primarily undergraduate, Hispanic-serving institution with no telescopes of its own. Exchanges of students between institutions for a several weeks or during summers would likely constitute something of a personal cultural renaissance for both for some Cal Poly Pomona students who have never left the greater LA area and some Wyoming students who have gown up in "towns" of <100 people! Impacts on teaching and research at Cal Poly Pomona and details of C–WARE are described in the RUI supplement portion of Co-PI Povich's companion proposal.

Funding of this program promotes local infrastructure at a rural institution where 37% of students are the first in their family to attend college by making excellent use of the mid-size WIRO telescope which is 100% owned and operated by the University of Wyoming (see Facilities and Resources section) and is located just 55 minutes from the UW campus. This facility enables dozens or even hundreds of nights of telescope access for long-term, large, and synoptic programs that would be unschedulable at most observatories. Thus, it constitutes nearly unique facility within U.S. astronomy infrastructure. For example, the PI's 8-year radial velocity spectroscopic survey program to measure binary characteristics of massive stars (described in Section 6) utilized over 280 nights at WIRO for a type of program that could only be completed by having long-term, flexible telescope access. Demonstration of continued scientific productivity translates to continued/increased support from the State of Wyoming and the University. Recent institutional measures of support are described in the Facilities section. WIRO is used by undergraduates nationwide during the Research Experiences for Undergraduates astronomy program each summer. Students at the Wyoming REU site observed at WIRO ~60 nights, (much of it as the observer-in-charge) in the four months of June and July of 2012 and 2013 alone! In an era of resource closures, supporting a state-funded telescope at a land-grant university enriches the whole community both by the unique science it enables and the student training that it promotes. WIRO is heavily used for both public tours during an annual open house and by 60 junior high students and pre/in-service teachers each summer as part of Kobulnicky's ten-day ExxonMobil Bernard Harris Summer Science Camp. Operating since 2010, the Camp is overseen by the Bernard Harris Foundation, which requires that Kobulnicky participate in seven days of pre- and post-camp STEM-related training with other nationwide camp directors each year. WIRO is the centerpiece of the Wyoming camp, supporting authentic science investigation by camp participants who use it obtain spectra of possible life-supporting stars as part of

their team research project.

With this proposal Kobulnicky is requesting a small amount of seed funding to add a Research Experience for Teachers component to existing summer REU and middle school science camp activities on the UW campus. This in-service teacher from the rural mountain west region would spend three weeks working with pre- and in-service teachers already part of the 16-person ExxonMobil Bernard Harris Summer Science Camp team that conducts a rigorous, interdisciplinary residential camp for 48 youth. Teacher participants cite learning from faculty and other teachers as equipping them for their academic year job. The teacher would also spend five weeks participating in research activities at the WIRO telescope with the PI, CoI, their students, and with REU summer students. They would be part of the team that is encouraged solves astrophysical problems as they train tomorrow's STEM leaders to solve problems pertinent to our nation and world. It is our goal that, like the NSF summer camp funding before it (see Section 6), this seed funding can be converted into sustainable private funding of a Research Experiences for Teachers program for similar purposes.

Povich would involve hundreds of Astro 101 (PHY 303) students at the Hispanic-serving Cal Poly Pomona in the new ***Zooniverse*** module for finding bowshock nebulae. Creating authentic science experiences for college students promotes STEM education and interest in science careers. It empowers underrepresented groups whose first experience in science is a collaborative endeavor that transcends national boundaries. Povich's prior experience integrating Milky Way Project science into a series of laboratory activities showed that this was the most popular aspect of the entire class in an Astro 101 type setting. Kobulnicky will have an opportunity to teach a new required freshman seminar class at Wyoming in the coming years, and this kind of authentic science component could be adopted from Cal Poly Pomona for use in a similar setting for non-majors and beginning STEM students alike.

Finally, our program seeks to provide fundamental data on stellar mass loss that will support many astrophysical sub-fields as diverse as stellar evolution, stellar populations, supernovae, gamma-ray bursts, and gravitational wave physics, and even galaxy evolution. Progress on single and binary-star evolution resulting from mass loss cuts across the Astronomy portfolio as an interdisciplinary endeavor.

6.0 Results from Previous NSF Support

*** NSF AST-0908249** $399,000 7/09 - 9/13 *Characterizing Companions of the Most Massive Stars* (PI Chip Kobulnicky at University of Wyoming)

Intellectual Merits: We conducted the most comprehensive and complete radial velocity survey of 114 massive stars in the Cygnus OB2 Association (earlier than B2) to date using 290 nights on the Wyoming Infrared Observatory (WIRO) 2.3 m telescope. We determined orbital parameters for over 45 OB systems, the most in any single cluster or association. We determined that the binary fraction is ~90% for massive stars, and that 45% of these are close companions that will interact and exchange matter over the lifetime of the stars. The fraction of light from secondary stars is ~16%. The distribution of orbital periods is flat in log(P) and the distribution of mass ratios, q, is nearly flat between q=0.2 and q=1.0. The series of papers from this work has well over 200 citations. These statistics provide raw data to inform predictions for cosmic rates of supernovae, gamma-ray bursts, as well as theories of massive star formation.

Broader Impacts: The 280 nights of observing and associated data analysis involved ~20 Wyoming undergraduates and nine NSF REU summer students, along with 7 graduate students who were part of the team which presented at eight domestic and international meetings. The program also helped demonstrate the vitality of WIRO and garner additional State of Wyoming resources to support the observatory from the UW Office of Research. The few thousand dollars of NSF funding used in this grant

to start a 3-day summer science camp for ~15 junior high students was leveraged into an $80,000/yr grant from ExxonMobil to run a 10-day science camp for 48 middle school youth each year since 2010. The ExxonMobil Bernard Harris Summer Science Camp has become one of the hallmark academic camps at UW, featuring a visit by former astronaut Bernard Harris (the first black astronaut to walk in space). The development of this program has helped Kobulnicky become proficient in STEM education for middle school youth and expand the STEM/career readiness programs in our rural region where 37% of college students are the first in their families to attend.
Products: Our team completed eight ApJ or AJ papers, six published as Kiminki et al. or Kobulnicky et al. over 2009--2013, with contributions to at least four other publications. Two more large manuscripts are near submission. Out ream presented results annually at AAS meetings and internationally in Belgium, Italy, and Spain at massive star symposia.

***NSF AST-0901646** $249,000 9/09 - 8/12 *Exploring Large-Scale Star-Forming Structures in the Milky Way* (NSF Astronomy & Astrophysics Postdoctoral Fellowship, PI Matthew S. Povich at the Pennsylvania State University)
Intellectual Merit Summary: The PI was an integral member of 2 major, international collaborative research efforts, the *Chandra* Carina Complex Project (CCCP) and the Massive Young Stellar Complex Study in Infrared and X-rays (MYStIX), and became a founding member and a key leader of a third, the MWP. CCCP and MYStIX provided comprehensive X-ray and IR analyses of the Great Nebula in Carina and 19 other massive Galactic star-forming regions, including cataloging and classifying tens of thousands of directly-imaged young stellar members of these regions. CCCP revealed a complex, multi-cluster structure with a distributed population within the Carina Nebula, built by widespread star formation over >10 Myr, and demonstrated that the region has already experienced supernovae. The MWP cataloged >5000 IR bubbles, most of them produced by massive or intermediate-mass stars. The PI also led several smaller-scale, related projects. Our analysis of the star-forming population in the M17 SWex IR dark cloud revealed a distributed mode of active intermediate-mass star formation in which massive star formation is suppressed and motivated the first-ever targeted *Chandra* X-ray observation of an IR dark cloud. We (collaboration with L. Chomiuk, now at Michigan State U.) synthesized existing literature to obtain a new, normalized estimate of the Galactic star formation rate (SFR), and reanalyzed multiwavelength data on individual star-forming regions, demonstrating how systematic uncertainties may lead to factors of 2–3 *underestimates* in widely-used galactic SFR diagnostics.
Broader Impact Summary: The first incarnation of the MWP involved >15, 000 volunteer citizen scientists representing 178 countries (Simpson et al., 2012). Prior to the worldwide release, 84 students in the PI's introductory astronomy course for non-science majors at Penn State tested the interface as part of a course module developed by the PI to tie modern astronomical research more closely to the classroom experience. This course module, the MWP Student Research Activity, was subsequently adopted and used by other instructors at Penn State and at several other universities in every term since MWP launched in Fall 2010.
Publications and Products: Work carried out by the PI while solely supported by this award resulted in 16 papers published in ApJS, AJ, ApJL, or MNRAS, including 4 papers led and one co-led (2 authors) by the PI and 4 papers currently in press for MYStIX. The PI and collaborators presented results at numerous national and international conferences, including a press conference on CCCP results at the Summer 2011 AAS meeting in Boston.